

REPORT DOCUMENTATION PAGE

AFRL-SR-AR-TR-07-0191

The public reporting burden for this collection of information is estimated to average 1 hour per response, including the time for gathering and maintaining the data needed, and completing and reviewing the collection of information. Send comments regarding this burden estimate or any other aspect of this collection of information, including suggestions for reducing the burden, to the Department of Defense, Executive Service and Communication, Washington, DC 20301-4070. Send all other correspondence regarding this collection of information to the Office of Management and Enterprise Services, Department of Defense, Washington, DC 20301-4070. Send all other correspondence regarding this collection of information to the Office of Management and Enterprise Services, Department of Defense, Washington, DC 20301-4070.

PLEASE DO NOT RETURN YOUR FORM TO THE ABOVE ORGANIZATION.

1. REPORT DATE (DD-MM-YYYY)		2. REPORT TYPE FINAL REPORT		3. DATES COVERED (From - To) 01 AUG 2006 - 31 JUL 2007	
4. TITLE AND SUBTITLE OPTICAL LOGIC WITH GAIN: PHOTONIC CRYSTAL NANOCAVITY SWITCHES				5a. CONTRACT NUMBER	
				5b. GRANT NUMBER F49620-03-1-0418	
				5c. PROGRAM ELEMENT NUMBER 2305/DX	
				5d. PROJECT NUMBER 61102F	
6. AUTHOR(S) DR SCHERER				5e. TASK NUMBER	
				5f. WORK UNIT NUMBER	
7. PERFORMING ORGANIZATION NAME(S) AND ADDRESS(ES) CALIFORNIA INSTITUTE OF TECHNOLOGY 1200 E CALIFORNIA BLVD PASADENA CA 91125-001				8. PERFORMING ORGANIZATION REPORT NUMBER	
9. SPONSORING/MONITORING AGENCY NAME(S) AND ADDRESS(ES) AF OFFICE OF SCIENTIFIC RESEARCH 875 NORTH RANDOLPH STREET ROOM 3112 ARLINGTON VA 22203 DR ROBERT BARKER/NE				10. SPONSOR/MONITOR'S ACRONYM(S)	
				11. SPONSOR/MONITOR'S REPORT NUMBER(S)	
12. DISTRIBUTION/AVAILABILITY STATEMENT DISTRIBUTION STATEMENT A: UNLIMITED					
13. SUPPLEMENTARY NOTES					
14. ABSTRACT In this final report, we will describe the experimental results and new design concepts that we have developed over the past 3 years. We compare several approaches that take advantage of the addition of gain to optical logic system, and describe methods for electronic control over that gain. Moreover, we show several strategies of introducing optical gain into complex all-optical logic systems and explore the ultimate operational speed of these switches. It is generally desirable to miniaturize optical logic system in order to enable their integration in large numbers, and the approaches taken during this project have been focused on lithographically connected devices that can be readily miniaturized and integrated in large numbers.					
15. SUBJECT TERMS					
16. SECURITY CLASSIFICATION OF:			17. LIMITATION OF ABSTRACT	18. NUMBER OF PAGES	19a. NAME OF RESPONSIBLE PERSON
a. REPORT	b. ABSTRACT	c. THIS PAGE			19b. TELEPHONE NUMBER (Include area code)

Final Report: AFOSR

POC: Gernot Pomrenke

Optical Logic With Gain

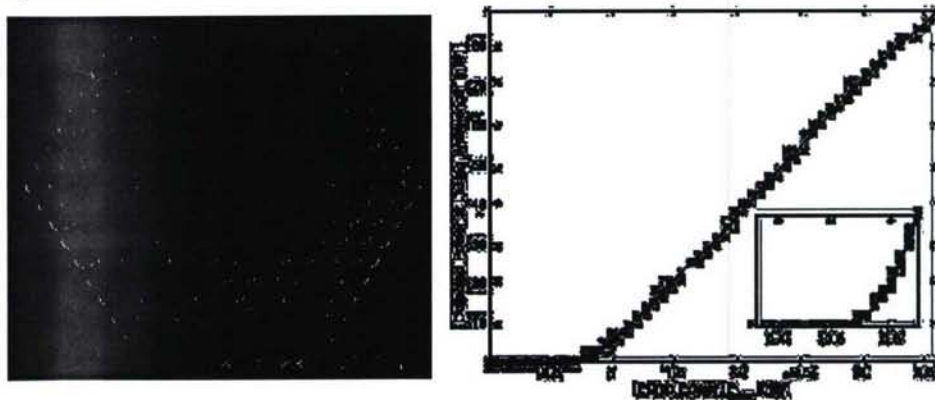
Axel Scherer, Caltech
Pasadena, CA 91125

Background

Over the past 40 years, the response frequencies of electronic logic gates has steadily increased towards 100 GHz and beyond, fueled by the trend towards miniaturization through ever-shorter gate length transistors. Ultimately, the frequencies of electronic logic systems are limited by the saturation velocities of carriers as well as prohibitive thermal loads. To solve this problem, architectures now favor the use of multiple computational strings and multi-core processors. In principle, even higher switching frequencies can be obtained by using light as the information medium and by building all-optical logic systems. In appropriately designed optical systems, much of the heat dissipation and signal lag problems plaguing electronic logic chips can be avoided, resulting in higher frequency responses and leading to Tera-Hertz frequency processors.

For the purpose of defining such complex optical logic systems, lithographically defined optical switches have in the past been coupled together on integrated photonic circuits. Unlike their electronic logic counterparts, all-optical systems are known to suffer from significant insertion losses which preclude cascading over many logic functions and have so far limited their application to rather simple signal processing tasks. The limited complexity of optical systems directly results from the tradition of using "passive" optical elements for the individual switches, resulting in a gradual loss of the initial number of photons inserted into the optical

Figure 1. Photonic Crystal Laser with L-L threshold curve showing nonlinear intensity behavior at threshold.



logic system, and a consequent deterioration of the signal to noise output of the processed optical signal. This is in very different from the propagation of electronic logic signals, which are typically regenerated through the addition of additional current at every logic node.

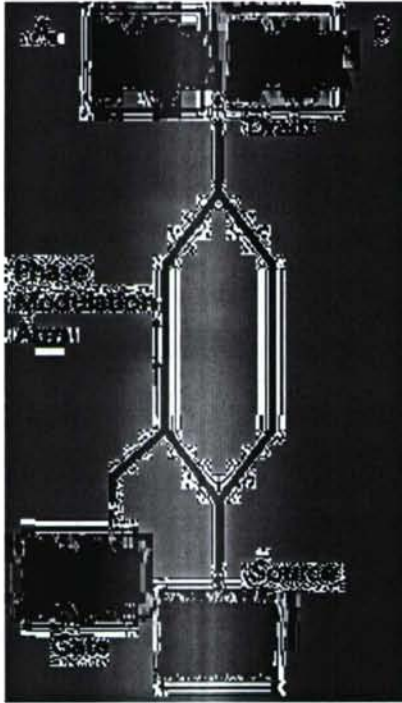


Figure 2. Schematic of a silicon/nonlinear polymer switch in which a gate signal switches a source signal

In the work completed under the AFOSR "Optical Logic with Gain" program, we have examined the concept of adding optical "gain" to all-optical logic systems and to mediate the inherent insertion losses in all-optical switching systems. We have designed two types of optical switches: (a) In the first kind of device, we add gain to the individual switching elements, two-dimensional photonic crystal nanocavities, by optically pumping these beyond laser threshold. Above the lasing threshold "knee", the ultra-small photonic crystal laser cavities can generate more light than is lost and thereby compensate for the insertion losses in the system. As a result of their small mode volumes, these lasers can be modulated at frequencies exceeding 100 GHz. (b) The second all-optical logic concept relied on using a passive all-optical system in silicon, in which additional photons are introduced at every node of the logic system. By using a smaller gating signal to modulate a larger switching signal, a system of passive devices can be connected together, each with "net signal gain". In many ways, this approach of adding new photons is very similar to the approach of adding current that is very common to the design of electronic logic systems.

In this final report, we will describe the experimental results and new design concepts that we have developed over the past 3 years. We compare several approaches that take advantage of the addition of gain to optical logic systems, and describe methods for electronic control over the gain. Moreover, we show several strategies of introducing optical gain into complex all-optical logic systems and explore the ultimate operational speed of these switches. It is generally desirable to miniaturize optical logic systems in order to enable their integration in large numbers, and the approaches taken during this project have been focused on lithographically connected devices that can be readily miniaturized and integrated in large numbers.

A. Photonic Crystal Nanocavity Switches

The ability to lithographically define high-finesse optical cavities within low surface recombination materials has enabled the optimization of photonic crystal lasers. In these lasers, slabs of high refractive index semiconductor containing efficiently emitting quantum wells are perforated with a lithographically defined Bragg reflection pattern that contains a small defect to form an optical nanocavity. Surprisingly, such cavities with mode volumes as small as 0.1 cubic half wavelengths can still support cavity Qs in excess of 10,000. The small mode volume leads to a geometric constraint of the light interaction within the cavity, and typical nanocavities only support one or two modes. As the speed and threshold of lasers typically depend on the number of modes that have to be pumped, it is possible to dramatically increase the switching frequency of lasers through miniaturization. By performing both frequency domain measurements followed by careful streak camera characterization, we have demonstrated optical switching at frequencies above 100 GHz within our photonic crystal nanocavities (Figure 3). We have also explore the use of nonlinear polymers included within the photonic crystal nanolasers. By designing optical cavities that retain their high Q values after back-filling with liquid crystal material, we have demonstrated Q-switching

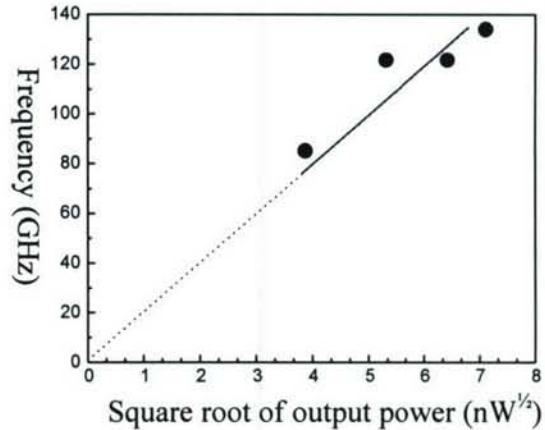


Figure 3. Frequency of laser switching versus injected power for a photonic crystal laser with mode volume of $0.3(n\lambda/2)^3$

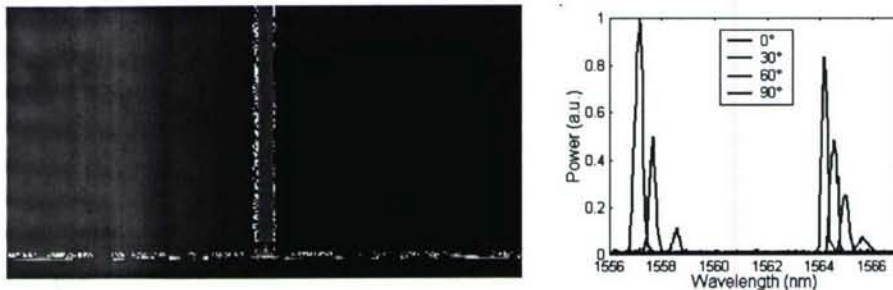


Figure 4. Modeling and experimental data of Q-switched photonic crystal laser in which the mode is switched with a nonlinear polymer included into the laser cavity. Note that almost 100% of the light is switched from one mode to another.

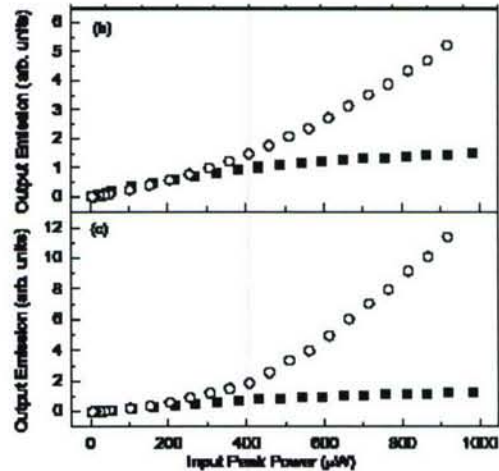
Another source of nonlinearity is obtained when introducing quantum dots within the optical cavities. We have demonstrated some of the first strongly coupled photon/cavity systems by using such quantum dot/ nanocavity devices. Nonlinear

behavior in these is dominated by quantum effects, potentially opening the possibility of developing alternative logic systems to the traditional classic switches (Figure 5).between two orthogonal modes with extraordinary efficiency (Figure 4).

Photonic crystal nanocavities were constructed both in InGaAsP/InP quantum well material emitting at 1550nm as well as in InGaP/InGaAlP material emitting at 640nm. Both materials systems exhibit low surface recombination velocities, but InGaAsP suffers from more Auger recombination than InGaP. Since the wavelength supported by the InGaAsP materials system is approximately 2.5 times larger than that in the InGaP system, and lithographic fabrication is consequently easier, it was initially advantageous to use this material system to define photonic crystal nanocavities. However, profound thermal management problems of laser operation at large duty cycles and the need for electrical pumping have provided technologically important limitations to the use of this materials system, and higher bandgap quantum well materials have become more attractive as an alternative to InGaAsP. As part of this project, we have constructed the first photonic crystal cavity lasers in the shorter wavelength visible material. This required an improvement of our lithographic fabrication control of a factor of ~2.5 (Figure 6).

The additional opportunity enabled by using the InGaP materials system is that it permits the use of higher quantum efficiency detectors and more compact optical systems. Indeed, streak camera measurements have benefited from the transition to more sensitive detector arrays. Another important opportunity provided by the InGaP materials system results from the ability to introduce large strain fields into the quantum well material during crystal growth. When the laser membrane is perforated, this in-grown strain is relaxed at the etched surfaces, and enormous strain fields can be obtained within the narrow semiconductor ribs that define the photonic crystal. This strain can be used to shift the bandgap of

Figure 5. (above) Lasing in InGaAs/GaAs quantum dot slabs in which approximately 80 quantum dots contribute to the laser emission. (below) electron micrograph of cavity array



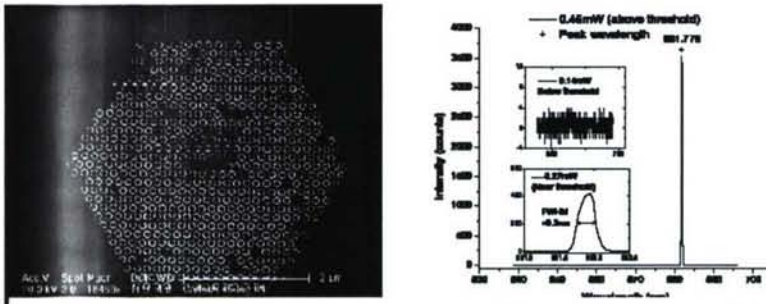


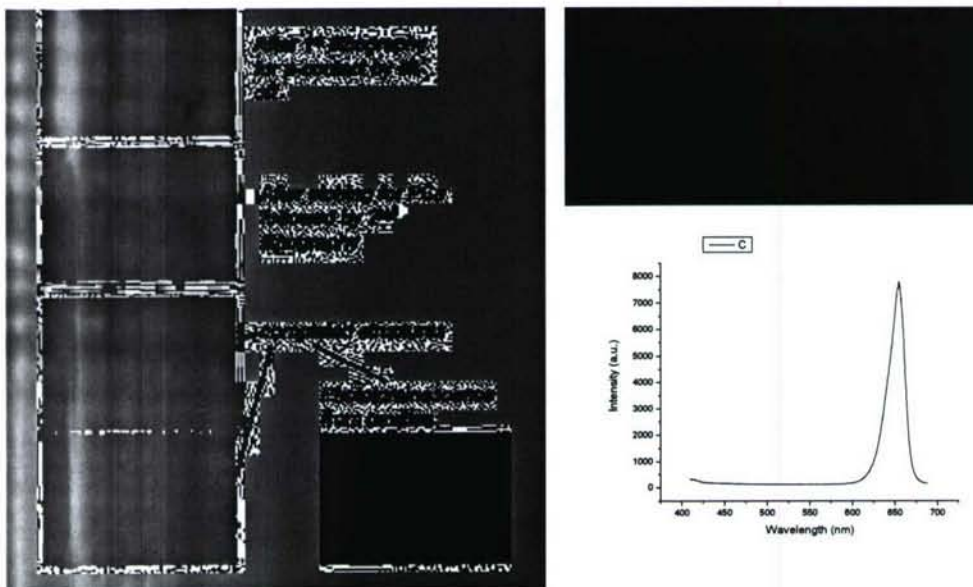
Figure 6. First InGaP photonic crystal laser emitting in the red (680nm) wavelength range.

the quantum well in the perforated material. Since the emitting material within the optical cavity is further away from a surface, it is possible to retain the high strain field within the cavity, and to establish a

laser in which light is not re-absorbed within the mirrors surrounding the optical nanocavity. As part of this program, we have designed photonic crystal lasers in which strain confinement helps to both reduce re-absorption losses and to avoid surface recombination of injected carriers. Indeed, this approach of strain confinement will yield a new class of extremely low threshold photonic crystal lasers.

Electrical pumping and addressing of photonic crystal lasers is essential for any complex application. Unfortunately, electrical pumping of photonic crystal lasers has so far only been demonstrated for a very short time by a group at KAIST in 2003, and has not been reproduced since. We have not yet been able to complete our goal of generating an electrically pumped photonic crystal nanolaser. However, we have come very close to achieving this goal and believe that we are on an excellent track to defining our first electrically pumped sources.

Figure 7. Electrically pumped InGaP nanocavities showing spontaneous emission (no lasing yet) at 650nm. The high quantum efficiency and low contact resistance are very promising indications that room temperature lasing is possible in these cavities.



By introducing p-n junctions within InGaAs quantum well materials and reducing the contact resistance to $50\mu\Omega/\text{cm}^2$, we have now completed the required electrical contacting scheme for successful cw lasing. Our first electroluminescence results are very encouraging, showing good quantum efficiencies and high brightness from InGaP material. The recipes developed under this AFOSR program will form the basis for defining robust photonic crystal lasers.

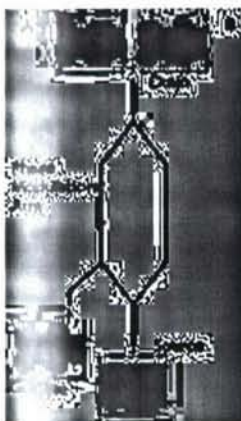
B. Silicon Nanophotonic Modulators and Switches

An alternative to introducing gain on the chip through light amplification relies on refreshing the on-chip signals by introducing light from a series of external "pump sources". This is analogous to the approach taken in electronic logic circuits, which rely on addition of currents at each logic node to regenerate the original signal strength. To accomplish this, it is necessary to switch a strong optical signal with a weaker one – i.e. to develop an all-optical switch that can function at the bit-rate of the logic system. During this AFOSR program, we have developed such switches and demonstrated their response speed up to frequencies of 2.6 THz. Mach-Zehnder interferometer geometries were chosen for our all-optical switches to modulate an incoming "optical power supply" signal with a "gating" signal that changes the optical path of one leg of the Mach-Zehnder and imposes the gating signal onto the new signal.



Figure 8. Image (above) and schematic cross-section (below) of a Silicon photonic waveguide with nonlinear polymer cladding

In this program, we designed and characterized waveguides with third harmonic nonlinearity by coating photo-refractive polymer onto a passive microfabricated silicon waveguide. Within this structure, it is possible to rapidly modulate the effective refractive index of the waveguide when the signal intensity is changed. In a Mach-Zehnder geometry, it is then possible to modulate an input signal with a high frequency gating signal. By beating the frequencies of two lasers, it was possible to generate frequencies of up to 2.6 THz, and these high-frequency signals were used to modulate the output intensity of the Mach-Zehnder device. It is very useful to lithographically miniaturize such devices, as it is then possible to connect these into more complex optical "circuits", which in turn enable optical logic on a chip.



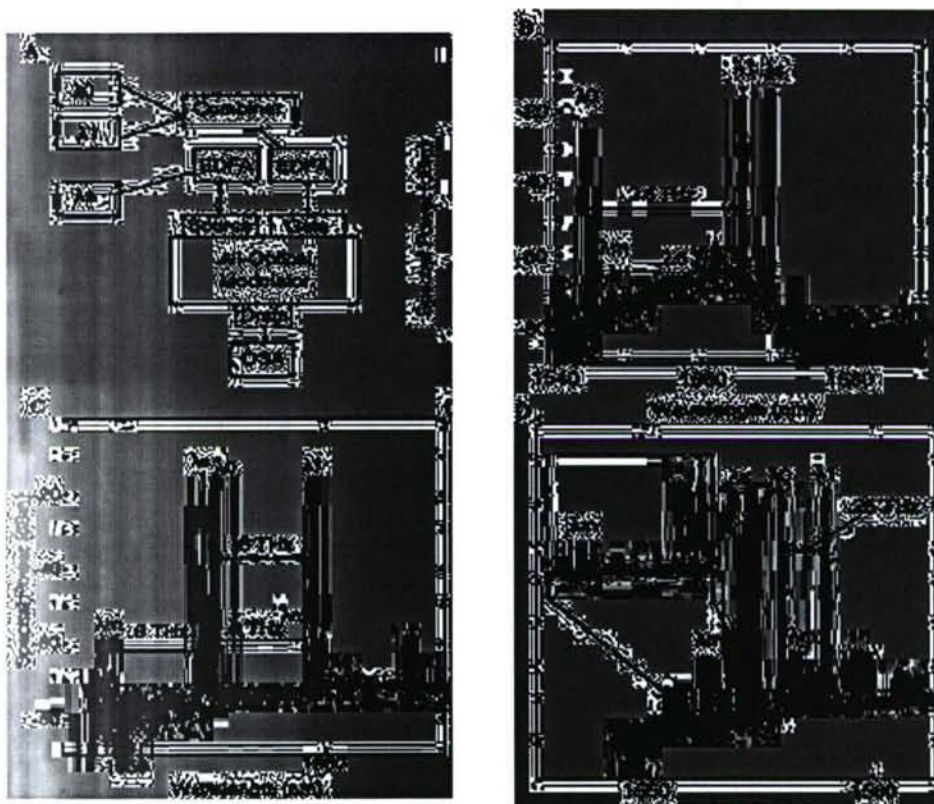


Figure 9. The logical diagram of the experiment. The spectral output in the optical-spectrum analyser for gate-laser spacings of 2.6 (b), 0.6 (c) and 0.25 (d) THz. The gate lasers are labelled l_0, l_1 ; the source signal is labelled l_s . In b, the relevant wavelength values are $l_0=1,544.3$ nm, $l_1=1,565.6$ nm and $l_s=1,569.3$ nm. The primary four-wave mixing sideband of the source signal is labelled l_m . Several other four-wave mixing peaks are visible. The inset in d shows the detail of the source and one set of sidebands as the former is tuned in increments of 0.2 nm. The change in the intensity of the central peak as the source wavelength is tuned, but not of the sidebands, is characteristic of the Mach-Zehnder interferometer's behaviour.

The advantage of this class of silicon photonic optical devices lies in their very fast response times, which is orders of magnitude above that of more conventional free carrier devices, and in the opportunity to use the high index contrast of the waveguides to miniaturize and couple many devices together.

Our preliminary results indicate that we can successfully modulate one optical signal with another at high frequencies. This is one very important step towards our ability to build optical logic devices and, ultimately, demonstrate "flip-flop" action. Much simpler devices, such as operational amplifiers, can now be contemplated and built to meet the challenging task of signal processing at THz frequencies. As a result of the AFOSR program on optical logic with gain, we now can solve some of the problems with storing information within optical circuits. The lack of optical bit storage has been one of the major impediments to

optical computation. We show that it is possible to reproduce an electronic flip-flop circuit within our new polymer-clad silicon waveguides to manipulate photons rather than electrons.

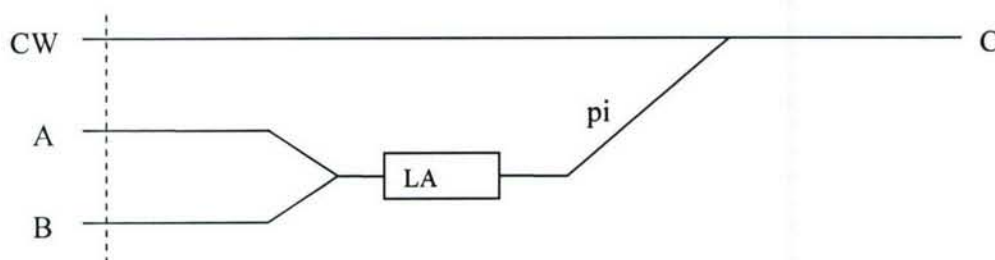
C. An Optical Flip-Flop

All digital logic operations can be performed with a NOR Operation

A	B	C
0	0	1
0	1	0
1	0	0
1	1	0

The optical logic proposed here can be implemented with interference of light with different phases in conjunction with a saturating linear optical amplifier. The required non-linearity is attained by the limiting amplifier (LA), and the logic is performed by interference of separate paths, all of which can now be implemented by using polymer clad silicon waveguides.

A basis NOR operations can be attained with the following geometry:

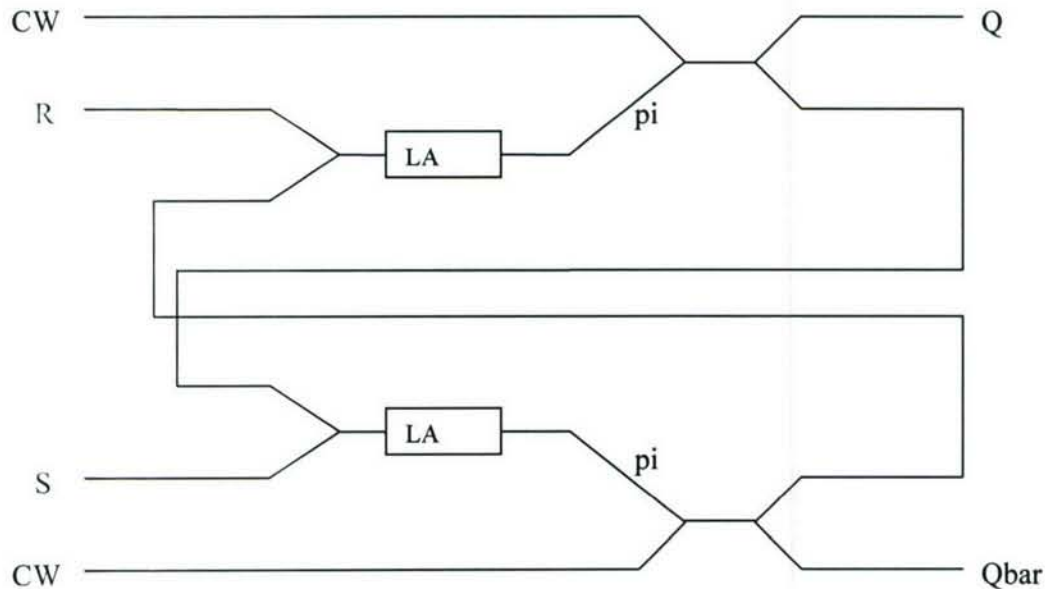


The three optical signals input at the left are a Continuous Wave (CW) light source, and two signal inputs, A and B. Presume all three signals are derived from the same source, and thus have the same wavelength and are coherent over a length much larger than the scale of the integrated circuitry. At the dashed line, all three paths are in phase, however, over the length of waveguide labeled "pi," the light from the input signals is delayed by pi radians, and is thus out of phase with the CW light at the Y-junction where they interfere. Also, the limiting amp is designed such that it saturates at a power level equivalent to the CW source.

Both output and input signals are defined by power levels, "0" when there is no light, and "1" when there is light.

When there is no signal at A or B, the CW light travels directly through to C (after sustaining losses at the Y junction). When light is input to either A or B, it is amplified to be at the same power level as CW, and subsequently interferes with CW to remove the signal at C. Thus, full NOR functionality is achieved.

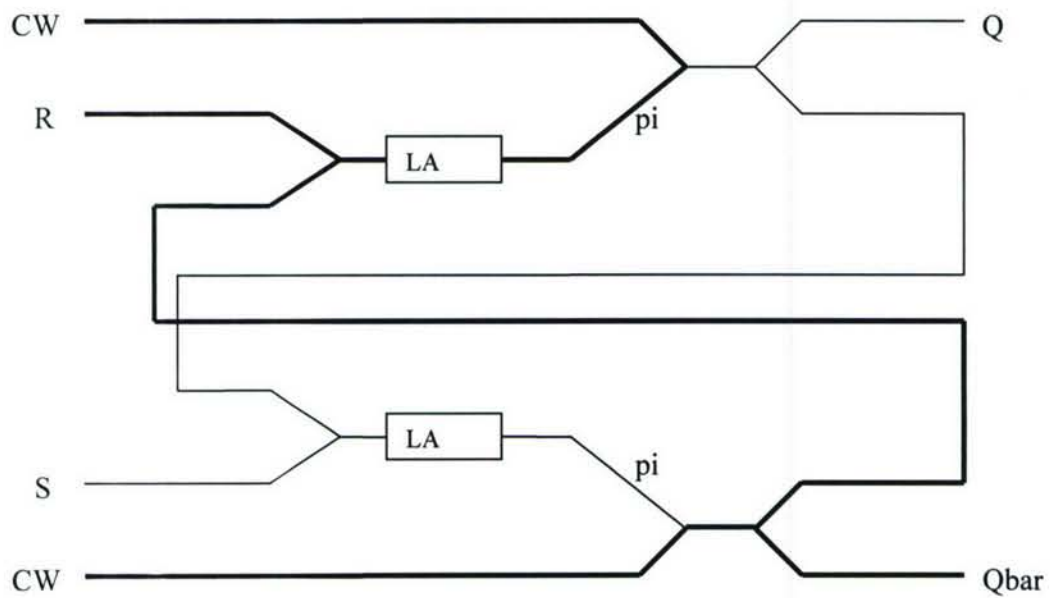
Now two of these structures can be combined to perform latching operations in the following geometry:



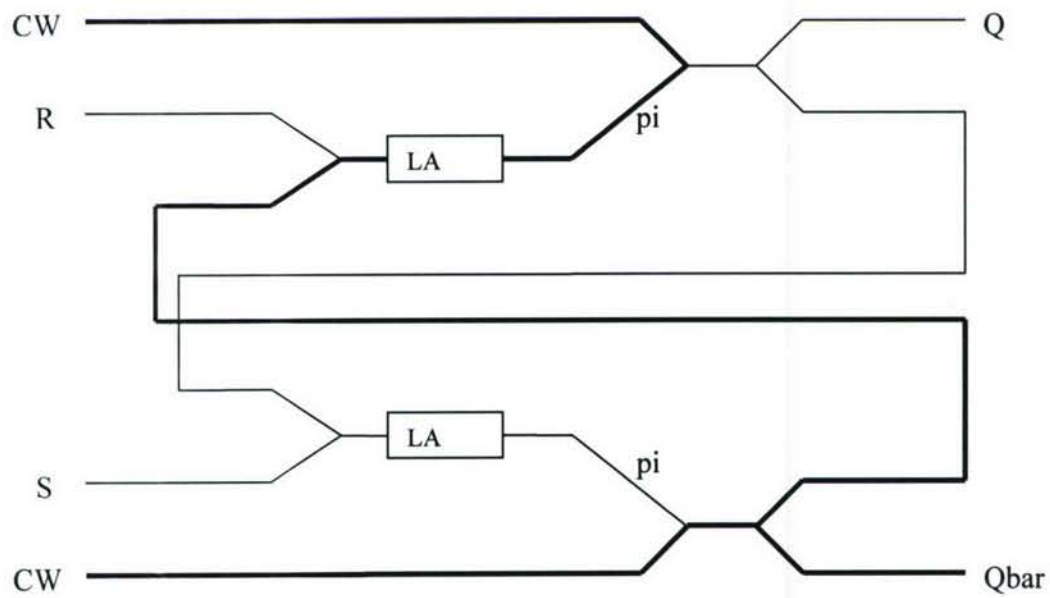
Note that the output is now sent to a splitter, where the power is divided. If power is output from the NOR, it will be fed back to the input of the other NOR, as well as being present at the output of the original NOR.

Like most simple latches, this latch has the potential to start up in an unstable state, or a random state. In order to start on a stable setting, either R or S must be set at the same time as the CW light is applied. For example, apply a signal at R at the same time as the two CW sources. The light from R will cancel the light at Q. The CW light from the bottom NOR will turn Qbar on and be fed back to the input of the top NOR, such that the signal from R can be removed and the system will stay in a stable state.

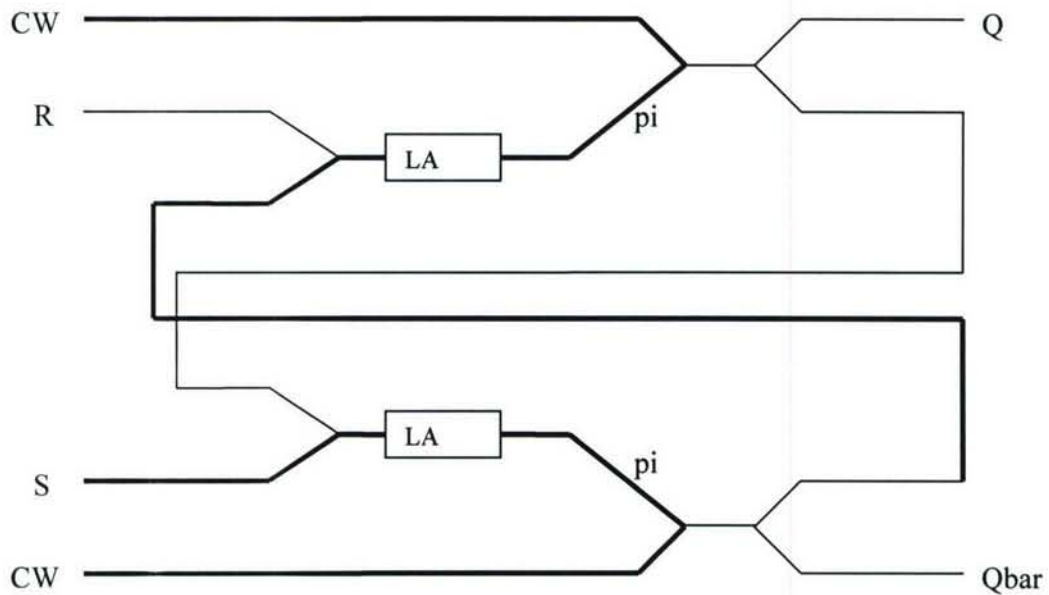
To set the latch, a signal is input to S, which will cancel the signal at Qbar and the feedback from the bottom NOR. This will end the cancellation of the top CW, creating a signal at Q, and a feedback for the bottom NOR. Once the signal reaches the bottom NOR, the signal from S can be removed and the circuit will remain in a stable state.



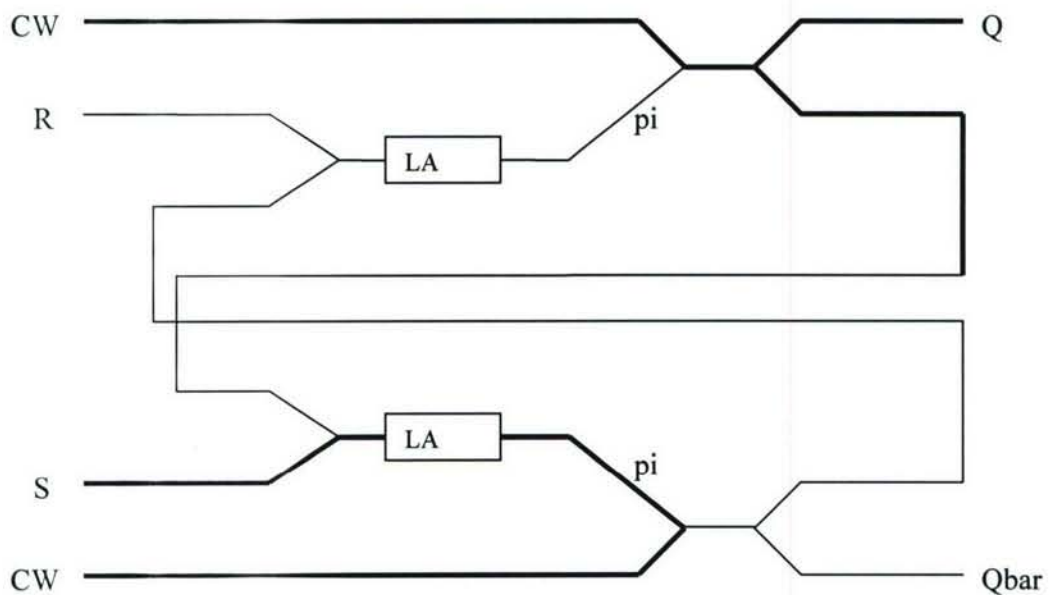
Light is input to both CWs and R for starting the latch



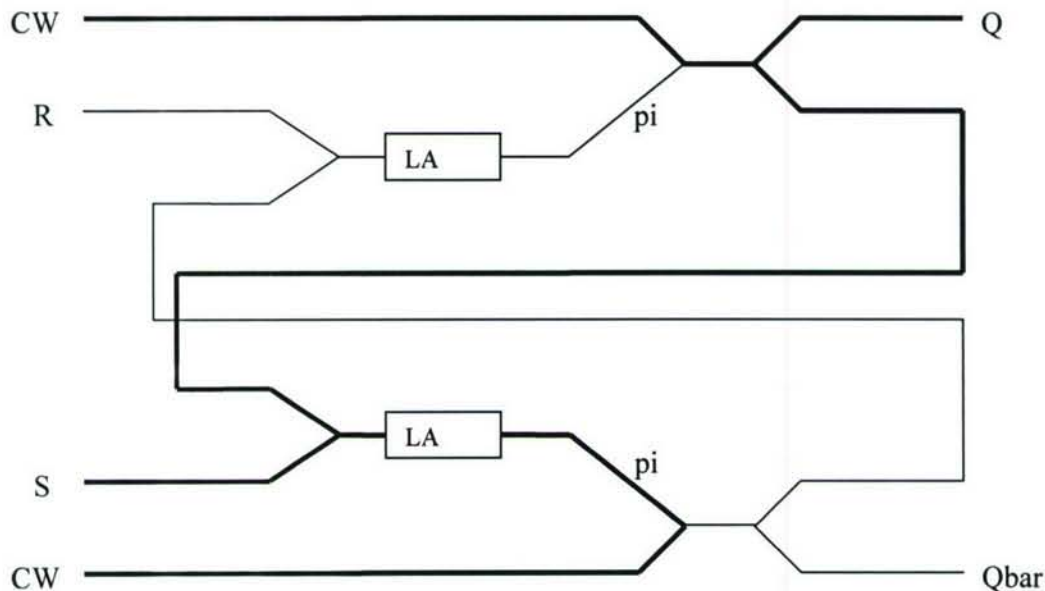
Input is removed from R, but the feedback from the bottom NOR keeps the circuit latched in the same state.



Now the signal applied at S has cancelled the signal output from the bottom NOR, and the trailing edge of the feedback pulse is shown.



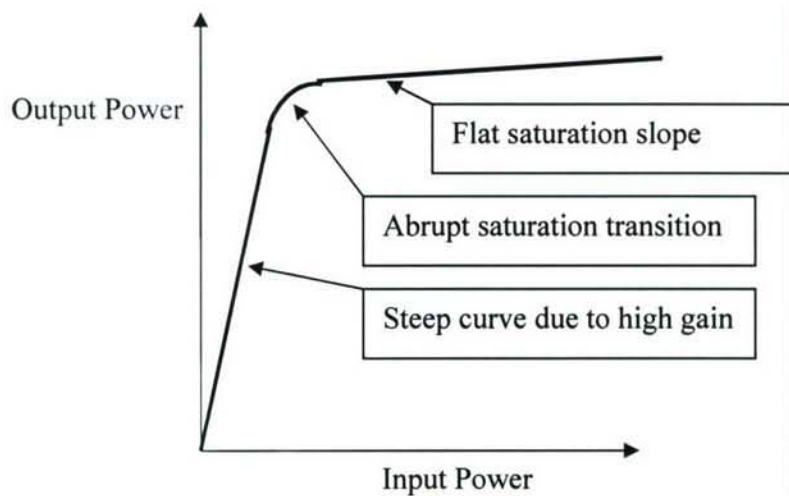
Now the feedback from the bottom NOR has disappeared, and there is no light canceling the signal from the top NOR, so Q is turned on, and feedback goes to the bottom NOR.



Now feedback from the top NOR reaches the bottom NOR allowing S to be removed, and completing the latching operation. Reset works the same way by applying a signal to R, canceling the light at the output of the top NOR, etc.

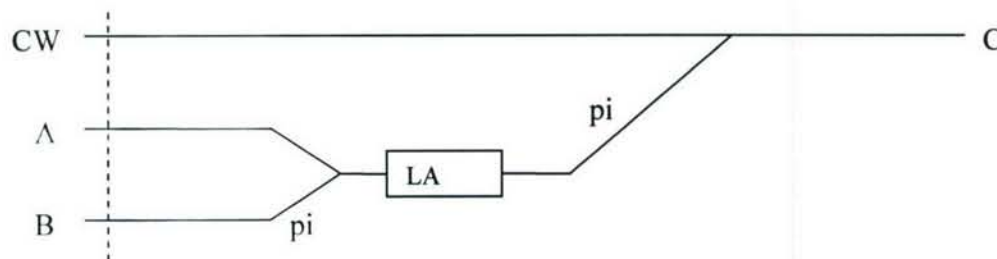
Note that the switching time is limited by the optical path length. With very short high index waveguides, the path length can easily be made using 5 micron bend radii for a total feedback path of 200 microns, and allowing a theoretical switching speed well into the 100s of Terahertz. However, it's unknown at this time how to achieve the required amplification with time delays that would make such switching practical. Speeds above 100 GHz are possible with pathlengths less than 3 mm, which should be possible with fully integrated circuitry. Note that large amounts of amplification are not necessary, only enough to compensate for the unavoidable scattering losses at the unbalanced Y-junctions. It's also a possibility to add LAs at the outputs and on the feedback arms to allow all LAs to have lower gain. Also note that the efficiency of the circuit would suffer when switching speeds start to limit the coherence length to the order of the length of the optical circuit. In addition, the ASE from any gain medium is detrimental to the performance, and would imply use of an optical filter which could ultimately limit bandwidth.

The ideal transfer function for a LA would be infinite gain, and an abrupt transition to an absolute saturation. While such an amplifier is hard to find, such a transfer function is not practically impossible, particularly with nonlinear polymer clad silicon waveguides, which give a very constant gain up to an abrupt saturation level.



The ideal LA transfer function. Note that it should be linear with respect to phase vs. frequency, and have no phase dependence on input power.

Note that it's possible to take this concept further and construct an optical comparator using a geometry similar to the original NOR, assuming again that the phases are constant at the dashed line.



In this case, a reference signal is input into A, and the signal to be tested is put into B, which is designed to have an additional π phase delay. If the power in A is greater than the power in B, the phase of the light output from the LA will have the phase of the original A, and will cancel the light out at C. If light input at B has more power than the light at A, then the light output from the LA will have the phase of B, and will instead constructively interfere at C.

Note that these proposals could be tested with an appropriate gain medium and simple fiber or free-space components, although the speed would be greatly reduced. Following proof-of-principle, it would be desired to implement the circuitry in a highly integrated fashion with short pathlengths. We have tested the speed of a 6 micrometer NOR gate by using a finite difference time domain code, and predict a lag time of below 100 femto-seconds (Figure 10).

Figure 10. Delay of an all-optical NOR gate. We used FDTD to implement 2D version of NOR gate, the necessary building block of digital logic. Input B is held at 0, while A is toggled from 0 to 1 to 0 at a bit rate of 1 THz, 50% duty cycle. The NOR gate is small – 25 x 6 microns as modeled

